Title
Generation and study of antibodies against two triangular trimers derived from Aβ

Journal
Peptide Science, 116(2)

ISSN
2475-8817

Authors
Kreutzer, Adam G
Malonis, Ryan J
Parrocha, Chelsea Marie T
et al.

Publication Date
2024-03-01

DOI
10.1002/pep2.24333

Peer reviewed

HHS Public Access

Author manuscript

Pept Sci (Hoboken). Author manuscript; available in PMC 2024 April 19.

Published in final edited form as:

Pept Sci (Hoboken). 2024 March ; 116(2): . doi:10.1002/pep2.24333.

Generation and Study of Antibodies against Two Triangular Trimers Derived from Aβ

Adam G. Kreutzer[a,†,*], **Ryan J. Malonis**[c,†], **Chelsea Marie T. Parrocha**[b], **Karen Tong**[c], **Gretchen Guaglianone**[a], **Jennifer T. Nguyen**[c], **Michelle N. Diab**[a], **Jonathan R. Lai**[c,*], **James S. Nowick**[a,b,*]

[a]Department of Chemistry, University of California Irvine, Irvine, CA 92697

[b]Department of Pharmaceutical Sciences, University of California Irvine, Irvine, CA 92697

[c]Department of Biochemistry, Albert Einstein College of Medicine, Bronx, NY 10461

Abstract

Monoclonal antibodies (mAbs) that target the P-amyloid peptide (Aβ) are important Alzheimer's disease research tools and are now being used as Alzheimer's disease therapies. Conformation-specific mAbs that target oligomeric and fibrillar Aβ assemblies are of particular interest, as these assemblies are associated with Alzheimer's disease pathogenesis and progression. This paper reports the generation of rabbit mAbs against two different triangular trimers derived from Aβ. These antibodies are the first mAbs generated against Aβ oligomer mimics in which the high-resolution structures of the oligomers are known. We describe the isolation of the mAbs using single B-cell sorting of peripheral blood mononuclear cells (PBMCs) from immunized rabbits, the selectivity of the mAbs for the triangular trimers, the immunoreactivity of the mAbs with aggregated $A\beta_{42}$, and the immunoreactivity of the mAbs in brain tissue from the 5xFAD Alzheimer's disease mouse model. The characterization of these mAbs against structurally defined trimers derived from Aβ enhances understanding of antibody-amyloid recognition and may benefit the development of diagnostics and immunotherapies in Alzheimer's disease.

INTRODUCTION

Understanding the structures of the toxic oligomers formed by the β-amyloid peptide (Aβ) is crucial for unravelling the molecular basis of Alzheimer's disease and for creating better Alzheimer's disease therapies.[1,2] Elucidating the structures of Aβ oligomers that form in the brain is challenging, because the oligomers are unstable and heterogeneous, constituting a multitude of assemblies that differ in size, stoichiometry, and morphology.[3] Furthermore, isolation of Aβ oligomers from brains yields miniscule quantities of material

*Corresponding authors: Adam G. Kreutzer, 4302 Natural Sciences 1, University of California Irvine, Irvine, CA 92697, Jonathan R. Lai, 1301 Morris Park Avenue, Room 519, Albert Einstein College of Medicine, Bronx, NY 10461, James S. Nowick, 4126 Natural Sciences 1, University of California Irvine, Irvine, CA 92697.

†These authors contributed equally to this work.

CONFLICT OF INTEREST STATEMENT

The Regents of the University of California has been assigned a United States patent for compounds reported in this paper in which A.G.K. and J.S.N. are inventors.

and is typically performed using buffers with high concentrations of detergents, which can alter the assembly state and structures of the oligomers.[4,5]

To gain insights into the structures of Aβ oligomers, researchers have prepared Aβ oligomers *in vitro* from synthetic or recombinantly expressed Aβ and then used low-resolution biophysical techniques, such as transmission electron microscopy, atomic force microscopy, gel electrophoresis, circular dichroism spectroscopy, infrared spectroscopy, and small-angle X-ray scattering to characterize the structures of these oligomers.[6,7,8,9,10,11,12,13,14] These *in vitro*-prepared Aβ oligomers have then been used as antigens to create antibodies, which are used as probes to correlate the structures of the oligomers prepared *in vitro* with oligomers in the brain.[15,16,17,18,19,20,21] While this "top-down" approach has yielded valuable insights into the conformations and structures of Aβ oligomers that form in the brain, the Aβ antigens used to generate many of these antibodies contain heterogenous oligomers with structurally undefined epitopes; thus, the structural insights obtained from this approach are limited.

We are developing a "bottom-up" approach for understanding the structures of Aβ oligomers that form in the brain using antibodies generated against Aβ oligomer mimics in which the high-resolution structures are known. This approach consists of: (1) design and synthesis of conformationally constrained Aβ β-hairpin peptides, (2) elucidation of the structures of the oligomers that the Aβ β-hairpin peptides form using X-ray crystallography, (3) design and synthesis of covalently stabilized Aβ oligomer mimics, (4) structural, biophysical, and biological characterization of the Aβ oligomer mimics, (5) generation of antibodies against the Aβ oligomer mimics, and (6) evaluation of immunoreactivity of the antibodies with full-length Aβ *in vitro* and Alzheimer's disease transgenic mouse brain tissue. Figure 1 illustrates this approach. Our working model is that antibodies generated against our covalently stabilized oligomers will provide greater insights into the structures of the Aβ assemblies in the brain, because the high-resolution structures of the epitopes on our oligomers are known.

We recently reported the structural, biophysical, and biological characterization of the Aβ oligomer mimics 2AT and KLT (Figures 2 and SI).[22,23] 2AT and KLT are covalently stabilized triangular trimers composed of different β-hairpin peptides derived from Aβ. 2AT is composed of three β-hairpin peptides in which $Aβ_{17–23}$ is across from $Aβ_{30–36}$; KLT is composed of three β-hairpin peptides in which $Aβ_{16–22}$ is across from $Aβ_{30–36}$. We elucidated the X-ray crystallographic structures of 2AT and KLT, and demonstrated through a series of biophysical and cell-based biological studies that the two trimers share characteristics with oligomers of full-length Aβ and differentially impact the aggregation and toxicity of full-length Aβ. We now report the generation and study of rabbit monoclonal antibodies (mAbs) against 2AT and KLT. Here, we describe: (1) isolation of the 2AT and KLT mAbs using single B-cell sorting of peripheral blood mononuclear cells (PBMCs), (2) the selectivity of the mAbs for the trimers 2AT and KLT, and (3) evaluation of the immunoreactivity of the mAbs against recombinantly expressed Aβ and brain tissue from the 5xFAD Alzheimer's disease mouse model.

MATERIALS AND METHODS

Peptide synthesis and purification.

2AT and KLT and their corresponding monomers 2AM and KLM were synthesized and purified as previously described.[22]

Rabbit immunization and bleeding.

Rabbits were immunized with 2AT and KLT by Pacific Immunology (Ramona, CA, www.pacificimmunology.com) using standard custom antibody production procedures approved by IACUC, and PBMCs were isolated from blood each production bleed and shipped on dry ice for single B-cell sorting. For the rabbit immunizations, 2AT and KLT were conjugated to the carrier protein keyhole limpet hemocyanin (KLH) using standard EDC conjugation chemistry. The EDC was obtained from Thermo Scientific (catalog # 22980) and the conjugations were performed according to manufacturer's instructions. Two New Zealand white rabbits were then immunized with the 2AT-KLH or KLT-KLH conjugates in complete Freund's adjuvant. The rabbits were boosted after ~21 days with the conjugates in incomplete Freund's adjuvant, and then boosted again ~21 days later. Production bleeds were performed 7 and 21 days after the second boost to yield ~25 mL of antisera from each rabbit. The rabbits were then boosted on a monthly schedule, with production bleeds occurring 7 and 21 days after each boost. The reactivity of polyclonal sera toward the antigens was confirmed by ELISA.

Biotinylation of 2AT and KLT.

Trimers 2AT and KLT were biotinylated using EZ-Link™ NHS-PEG4-biotin (Thermo Scientific™, catalog # A39259). To begin, 3 mg portions of 2AT and KLT as the TFA salts were weighed into 1.7 mL microcentrifuge tubes and dissolved in 100% DMSO. 50 molar equivalents of A,A-diisopropylethylamine was then added to the trimer solutions. A pre-weighed 2 mg aliquot ofNHS-PEG4-biotin was then dissolved with 100 μL DMSO, and then 1.75 molar equivalents were added to the trimer solutions. The reaction mixtures were incubated at room temperature on tube rotator for 2 hours. The reaction mixtures were then immediately subjected to reverse-phase HPLC (RP-HPLC). RP-HPLC was performed using an Agilent Zorbax 300SB-C18 semi-preparative column (21.2 mm × 250 mm, 7 pm particle size) with an Agilent Prep 100 A C18 guard column (21.2 mm × 10 mm) on a Rainin Dynamax HPLC with a flow rate of 20.0 mL/min and eluted with a gradient of 20–45% CH_3CN over 90 min. Fractions were collected, combined, and then analyzed by LC-MS on an ACQUITY UPLC H-class system, Xevo G2-XS QTof (Waters Corp.) equipped with a Protein BEH C4 column (300 Å, 1.7 μm, 2.1 mm X 50 mm, Waters Corp).

Isolation of rabbit mAbs.

Rabbit mAbs were generated using a single B-cell cloning strategy similar to those previously described.[24,25] Antigen-reactive B cells were isolated from rabbit PBMCs by fluorescence-activated cell sorting. Rabbit PBMCs were stained with the following fluorophore-conjugated rabbit-specific antibodies: CD4 (FITC), CD8 (FITC), IgM (FITC), and IgG (Alexa 680). The viable cell population was detected using LIVE/DEAD

(ThermoFisher) staining. Biotinylated 2AT and KLT were incubated with stained PBMCs at a concentration of 400 nM and subsequently labeled with streptavidin-conjugated phycoerythrin (PE) (Life Technologies). Viable cells that were antigen^{+} IgG^{+} CD4/CD8/IgM^{-} were sorted into single PCRtubes, and cDNA was synthesized by RT-PCR. Nested PCR was performed with an adapted set of rabbit IgH- and IgK-specific primers[26,27] to amplify rabbit variable domain fragments, which were then cloned into the pMAZ vector[28] containing human IgGl constant domains. Sequences were analyzed using the IMGT/V-quest tool.[29] The mAb plasmids were transiently transfected in FreeStyle 293F cells or ExpiCHO cells as per the manufacturer's protocol, and antibody purified by protein A chromatography. Fab constructs containing a C-terminal His tag on the heavy chain were transiently transfected in ExpiCHO cells as per the manufacturer's protocol and purified by Ni-NTA affinity chromatography.

ELISA screening of the 2AT and KLT mAbs.

Antibody binding was determined by ELISA with either immobilized antigen or immobilized antibody. High binding 96-well plates (Costar) were coated with 100 ng of 2AT or KLT peptide or 200 ng of mAb. Wells were blocked with 1% bovine serum albumin (BSA) for 2 h at room temperature and washed five times with phosphate-buffered saline (PBS)-T (PBS pH 7.4, 0.05% Tween-20). For immobilized antigen ELISA, isolated mAbs were diluted in PB-T (PBS pH 7.4, 0.2% BSA, 0.05% Tween) at 10 nM, 1 nM and 0.1 nM concentrations and incubated for 1 h at 37 °C. Plates were washed, and protein A conjugated to horseradish peroxidase (HRP) (Life Technologies) was added atal:2,000 dilution. For immobilized antibody ELISA, biotinylated 2AT or KLT was diluted to 30 nM, 10 nM, and 1 nM in PB-T, incubated for lhat37 °C, washed, then detected with streptavidin-HRP (Life Technologies) at a 1:10,000 dilution. After 1 h incubation at 37 °C, plates were washed and developed using TMB (Thermo Fisher Scientific) and absorbance at 450 nm was measured on Synergy H4 Hybrid reader (BioTek).

Indirect ELISA of the 2AT and KLT mAbs against 2AM, 2AT, KLM, and KLT.

Indirect ELISA was used to determine the selectivity of the 2AT and KLT mAbs for the compounds 2AM, 2AT, KLM, and KLT. Three technical replicates were performed for each experiment. Each aspiration and washing step in the ELISA procedure was performed using a Fisherbrand™ accuWash™ Microplate Washer (catalog # 14–377-577).

To coat the wells of the ELISA plates, 10 mg/mL stock solutions of the compounds as TFA salts were prepared gravimetrically by dissolving 1.0 mg of each compound in 100 pL of deionized water that had been passed through a 0.2 μm filter. 1 μg/mL solutions of the compounds were then prepared by adding 1 μL of the 10 mg/mL stocks to 10 mL carbonate buffer (15 mM Na_2C0_3, 35 mM $NaHC0_3$, 0.02% (w/v) sodium azide, pH 9.5). The 1 μg/mL solutions of the compounds were then poured into reagent reservoirs and a multichannel pipette was used to transfer 50 pL to the appropriate wells of a Thermo Scientific™ Maxisorp 96-well plate (catalog # 12–565-135). Each well contained a total of 50 ng the compounds. 2AM was added to all wells in columns 1–3, 2AT was added to all wells in columns 4–6, KLM was added to all wells in columns 7–9, KLT was added to all wells in columns 10–12. The 96-well plate was then sealed with an adhesive 96-well plate

seal (Axygen, catalog # PCR-SP) and incubated overnight (~16 hours) at room temperature on a rotating shaker set to 90 RPM.

The next day, 20 mL of 1% BSA was prepared by adding 200 mg of BSA (Fraction V) (Fisher BioReagents™, catalog # BP1600–100) to 20 mL PBS. The solutions of 2AM, 2AT, KLM, and KLT were aspirated from the wells of the 96-well plate and then washed lx with PBST (10 mM Na2HP04, 1.8 mM KH_2PO_4, 137 mM NaCl, 2.7 mM KC1, 0.5% Tween-20). Next, a multichannel pipette was used to transfer 75 µL of 1% BSA to each well, the plate was sealed, and incubated for at least 1 hour at room temperature on a rotating shaker set to 90 RPM to block uncoated sites in the wells. During the last 15 minutes of the blocking step, 3 µg/mL solutions of each mAh were prepared in 1% BSA. When the blocking step was complete, the wells were aspirated and washed 3x with PBST. Using a multi-channel pipette, 50 µL of 1% BSA was then added to the wells in the bottom seven rows of the 96-well plate (rows B–H). 75 µL of the 3 µg/mL mAh solutions was then added to the wells in the top row (row A). A multi-channel pipette was then used to create a three-fold serial dilution series of each mAh The 96-well plated was then sealed with an adhesive plate seal and incubated for 2 hours at room temperature on a rotating shaker set to 90 RPM.

After the 2-hour incubation, the mAh solutions were aspirated and the wells were washed 3x with PBST. A 50 µL portion of AffiPure Goat Anti-Human Fey conjugated to horse radish peroxidase (GαH-HRP; Jackson ImmunoResearch, catalog # 111–035–144) diluted 1:10,000 in 1% BSA was then added to each well. The 96-well plated was then sealed with an adhesive plate seal and incubated for 1 hour at room temperature on a rotating shaker set to 90 RPM.

After the 1-hour incubation, the GαH-HRP solution was aspirated and the wells were washed 3x with PBST. A 50 pL portion of 3,3’,5,5’-tetramethybenzidine (TMB) (Millipore Sigma, catalog # ES001–500ML) was then added to each well and allowed to react until the blue color reached a sufficient hue. A 50 µL portion of 1 M aqueous HC1 was then added to each well to quench the reaction and the absorbance was measured at 450 nm using a MultiSkan GO plate reader. The absorbance readings for the three replicates were averaged and the standard deviations were calculated using GraphPad Prism. The data were then plotted and fit using the equation “Specific binding with Hill slope” in GraphPad Prism to estimate the EC_{50} values for each mAh against each compound.

Dot blot assays of the 2AT and KLT mAbs with $A\beta_{42}$.—A 1 mg portion of recombinantly expressed $A\beta_{42}$ as the ammonium salt was purchased from rPeptide (catalog # A-1167–2) and received as a fluffy lyophilized solid in a glass amber vial. The 1 mg $A\beta_{42}$ portion was dissolved with 1 mL of 2 mM NaOH to create a 1 mg/mL $A\beta_{42}$ solution. The 1 mg/mL $A\beta_{42}$ solution was then sonicated in a water bath sonicator for 5 minutes. After sonication, 0.02 µmol aliquots of $A\beta_{42}$ were prepared by transferring 92.6 µL portions of the 1 mg/mL $A\mu_{42}$ solution to low-binding microcentrifuge tubes (Axygen, catalog # MCT-175-L-C) containing a hole in the lid of the tube created by puncturing the lid with a 22 gauge needle. The aliquots were then frozen on dry ice for 1 hour, transferred to a lyophilization vessel, and lyophilized overnight. The next day, the aliquots were removed from the lyophilizer and each microcentrifuge tube was immediately transferred to a 50 mL

conical tube. The 50 mL conical tubes were sealed by tightening the lid and stored at −80 °C until use.

For the dot blot assays, an aliquot of $A\beta_{42}$ was removed from the −80 °C freezer and allowed to equilibrate to room temperature. The pellet was then dissolved in 92.6 μL PBS to create a 1 mg/mL solution of $A\beta_{42}$. 1 μL portions of the $A\beta_{42}$ solution were then immediately spotted onto the nitrocellulose membranes, constituting the “0-minute” time points. The $A\beta_{42}$ solution was then incubated at room temperature under quiescent conditions, and 1 μL portions of the $A\beta_{42}$ solution were spotted every 45 minutes up to 180 minutes. After the $A\beta_{42}$ from the 180-minute time point was spotted, a 1 μL portion of a 1 mg/mL $A\beta_{42}$ solution created 96 hours prior was then spotted. The membrane was allowed to dry for 30 minutes, and then standard immunoblotting was performed as follows.

Non-reactive sites were blocked on each membrane by rocking the membranes in 5% (w/v) non-fat powdered milk in low-Tween TBS (TBS-1T: 50 mM Tris buffer pH 7.4, 150 mM NaCl, 0.01% Tween 20) for lh at room temperature. The membranes were then incubated while rocking overnight at 4 °C in each mAh (3 μg/mL) or 6E10 (3 μg/mL) prepared in the 5% milk solution. The next day, the membranes were washed with 3x TBS-1T for 5 minutes. The mAb-exposed membranes were then treated with a solution of goat anti-human IgGFc-HRP antibody (1 μg/mL) (Jackson ImmunoResearch catalog # 111–035-144); the 6E10 membrane was treated with a solution of goat anti-mouse IgG HRP antibody (0.8 μg/mL) (Jackson ImmunoResearch catalog # 115–035-062) for 1 hour at room temperature. The membranes were then washed 3x with TBS-1T for 5 min. Thermo Scientific SuperSignal™ West Pico PLUS Chemiluminescent Substrate (catalog # 34580) was prepared according to the manufacturer’s instructions and supplemented with Thermo Scientific SuperSignal™ West Femto Maximum Sensitivity Substrate (catalog # 34095) and then 5 mL of the prepared substrate was added to each membrane. The membranes were incubated in the HRP substrate for ~5 min before imaging. The membranes were imaged using a Bio-Rad ChemiDoc Gel Imaging System.

Safety statement.—There were no unexpected, new, and/or significant hazards or risks associated with the reported work.

RESULTS AND DISCUSSION

Generation and isolation of rabbit monoclonal antibodies against 2AT and KLT.

We sought to isolate 2AT- and KLT-specific antibodies from immunized rabbits to explore antibody-trimer interactions and to develop probes to understand the relationship between 2AT and KLT and oligomers formed by full-length Aβ *in vitro* and *in vivo.* Rabbits were selected for immunization, because they harbor a distinct antibody repertoire that can mount a robust immune response against diverse antigens, particularly with respect to small peptide epitopes.[30,31] Rabbits were immunized with 2AT and KLT conjugated to the carrier protein keyhole limpet hemocyanin (KLH) in Freund’s adjuvant. The rabbits produced high serum antibody titers to both the 2AT and KLT antigens, as assessed by ELISA of the polyclonal antisera.

For isolation of 2AT and KLT mAbs, 2AT and KLT were first conjugated to biotin using an NHS-activated biotin bearing a PEG4 linker (NHS-P4B) to create the 2AT-PB and KLT-PB conjugates.[25] We used 1.75 equivalents of NHS-P4B to minimize excessive modification of potential epitopes on the trimers. The biotinylation reactions produced mixtures of multiple-biotinylated species with double-labeled species predominating (Figure S2). We used the mixture of biotinylated species in the single B-cell sorting. To isolate mAbs that target 2AT, a single B-cell sorting strategy using rabbits immunized with 2AT was employed (Figure 3). PBMCs were isolated and sorted for individual 2AT-reactive B cells by fluorescence-activated cell sorting (FACS). First, PBMCs were sorted for size/granularity consistent with lymphocytes (Figure 3A). Since rabbit B cells contain fewer apparent cell-surface markers than mouse or human B cells, a wide negative selection was done to deplete the population of undesired non-viable cells such as CD4 and CD8 T cells, and IgM^+ B cells. Subsequent positive gating for $2AT^+$ IgG^+ B cells was done and individual cells in this population were sorted into wells. After lysis and cDNA synthesis, variable heavy and kappa light domains were amplified using a nested PCR strategy with an adapted primer cocktail that targets the leader sequence and constant region of the rabbit Ig gene. In wild type rabbits, > 70% of antibody light chains originate from the kappal locus, while the remaining antibody light chains are from the kappa2 and lambda loci. The recovered variable domains were then cloned as recombinant chimeric rabbit-human IgGl antibodies and expressed on small- to mid-scale in HEK293F or ExpiCHO cells and then purified for initial analysis.

Twenty-eight 2AT mAbs were successfully expressed and screened for reactivity toward 2AT by two different ELISA experiments. In the first ELISA experiment, unlabeled 2AT was coated on the plate, three different concentrations of each mAb were then added, and the bound mAbs were detected with protein A-HRP (Figure 3B, left). In the second ELISA experiment, each mAb was coated on the plate, three different concentrations of 2AT-PB were then added, and the bound 2AT-PB was detected with streptavidin-HRP (Figure 3B, right). These two different ELISA experiments were done in parallel to test specific reactivity toward both immobilized and free 2AT, and to exclude mAbs that reacted with the PEG-biotin linker. Eighteen mAbs showed strong reactivity with 2AT in both ELISA experiments and were selected for further characterization. Sequence analysis of these mAbs showed diversity among the VH and V kappa gene lineages, with IGHV1S34 and IGKV1S10 most abundant (Figure 3C). The HCDR3 length ranged from 9 to 13 residues and the LCDR3 length ranged from 11 to 14 residues (Figure 3D). KLT-specific rabbit mAbs were isolated using a similar protocol. Fifteen KLT mAbs were successfully expressed, with 9 exhibiting strong reactivity toward KLT (Figure 4). Through these ELISA screening experiments, a total of 27 mAbs (18 2AT mAbs and 9 KLT mAbs) were selected for further characterization.

Selectivity of the 2AT and KLT mAbs.

The Aβ oligomer models 2AT and KLT each display unique epitopes, as well as epitopes that are not unique. Identifying mAbs that are selective for the unique epitopes is important for exploring the relationship between these Aβ oligomer models and full-length Aβ. To identify mAbs that recognize unique epitopes, we first screened mAbs for cross-reactivity among 2AT and KLT, and then for selectivity toward their cognate trimers over

corresponding monomers. We used indirect ELISAs to measure the binding of each of the 27 mAbs to 2AT and KLT and their corresponding monomers 2AM and KLM to identify mAbs that are selective for epitopes unique to the trimers (Figure 5). Figure SI shows the chemical structures of 2AT, KLT, 2AM, and KLM. To perform these ELISA experiments, equal amounts (50 ng) of 2AT, KLT, 2AM, or KLM were applied to the wells of an ELISA plate. Serial dilutions of each mAb were then added to the wells, followed by a secondary antibody conjugated to horseradish peroxidase (HRP). The half-maximal effective concentration (EC_{50}) of each mAb was then determined for 2AT, KLT, 2AM, and KLM (Figure 5B).

The ELISA experiments reveal that there is little or no cross-reactivity between the 2AT mAbs and KLT or between the KLT mAbs and 2AT, with almost all the mAbs exhibiting 100- to 1000-fold greater selectivity for their cognate trimer (Figures 5A and B). In most cases, the binding of the mAbs to the non-cognate trimers and monomers was so weak that the EC_{so} values could not be determined (n.d.). These findings demonstrate that 2AT and KLT display dissimilar epitopes with little structural or conformational overlap, despite the two trimers being morphologically similar and sharing extensive amino acid sequence homology. These findings also support the approach of using antibodies to investigate the relationship of each trimer to oligomers of full-length Aβ, as each trimer promotes the production of mAbs that are highly selective for epitopes on that trimer.

Comparison of the EC_{50} values of each mAh for its cognate trimer and corresponding monomer revealed that some mAbs are more selective for the trimers than their corresponding monomers (Figure 5B). We quantified the selectivity of each mAh for its cognate trimer by calculating the quotient of the EC_{50} values for the monomer and the trimer. For example, the selectivity of RB2AT_87 was determined to be 10.0, the quotient of 0.8 nM (EC_{50} for 2AM) and 0.08 nM (EC_{50} for 2AT) (Figure 5A). The selectivity analysis reveals that six out of the eighteen 2AT mAbs exhibit greater than fivefold selectivity for trimer 2AT, and three out of the nine KLT mAbs exhibit greater than fivefold selectivity for trimer KLT (Figures 5C and D). These findings indicate that many of the mAbs in both panels are selective for epitopes that are unique to either the 2AT or KLT trimers.

Immunoreactivity of the 2AT and KLT mAbs with $A\beta_{42}$.

To investigate the relationship between 2AT and KLT and assemblies of full-length Aβ, we performed dot blot assays on 2AT and KLT mAbs that exhibited greater than fivefold selectivity for their cognate trimers. We used the anti-Aβ antibody 6E10 as a positive control. For this dot blot experiment, we aggregated recombinantly expressed $A\beta_{42}$ over time in PBS and spotted aliquots of the aggregated $A\beta_{42}$ on a nitrocellulose membrane every 45 minutes for a total of 180 minutes. We also spotted $A\beta_{42}$ that was aggregated for 96 hours. At the 0-minute time point, the population of $A\beta_{42}$ species applied to the membrane should be predominantly monomeric. As the aggregation time increases, the equilibrium shifts toward oligomeric and fibrillar aggregates.[32] At the 96-hour time point, the predominant species should be mature $A\beta_{42}$ fibrils, with little or no monomeric or oligomeric $A\beta_{42}$ left in solution.

The dot blots reveal that the 2AT and KLT mAbs exhibit varying levels of immunoreactivity with $A\beta_{42}$, with many of the mAbs showing some selectivity for aggregated Aβ42 (Figure 6). RB2AT_120 exhibits the strongest binding to $A\beta_{42}$, binding $A\beta_{42}$ comparably at all the early time points (0–180 minutes) but showing no selectivity among any of these time points (Figure 6A). RB2AT_120 exhibits weaker binding to mature $A\beta_{42}$ fibrils than the $A\beta_{42}$ species formed during the earlier time points, suggesting that this mAh binds an epitope on $A\beta_{42}$ that is structurally and conformationally distinct from epitopes on $A\beta_{42}$ fibrils. In contrast, RB2AT_167 exhibits stronger binding to mature fibrils than $A\beta_{42}$ assemblies formed at the earlier time points, suggesting that this mAh binds an epitope unique to mature fibrils (Figure 6A). RBKLT_20, RBKLT_16, RB2AT_52, RBKLT_14, and RB2AT_87 exhibit little or no binding to $A\beta_{42}$ at the 0-minute time point but weakly bind aggregated $A\beta_{42}$ at the later time points, showing comparable selectivity for early $A\beta_{42}$ aggregates and mature $A\beta_{42}$ fibrils (Figure 6B). RB2AT_64 and RB2AT_3 comparably bind $A\beta_{42}$ at all the time points examined, suggesting that these mAbs bind a generic $A\beta_{42}$ epitope. The positive control anti-Aβ antibody 6E10 exhibits strong binding to $A\beta_{42}$ at each time point (Figure 6D).

Immunoreactivity of the 2AT and KLT mAbs with 5xFAD mouse brains.

To better understand the relationship between 2AT and KLT and Aβ assemblies that form in the brain, we evaluated the immunoreactivity of RB2AT_120 and RB2AT_167 with brain slices from the Alzheimer's disease mouse model 5xFAD. We also evaluated additional 2AT mAbs and KLT mAbs that exhibited greater than fivefold selectivity for the trimers. For these studies, we stained brain slices from an 8-month-old female 5xFAD mouse with each mAb and the anti-Aβ antibody 6E10 using standard fluorescence-based immunostaining procedures, and then used fluorescence microscopy to image the brain slices. Fluorescence microscopy of the immunostained brain slices revealed than none of the 2AT or KLT mAbs that were studied exhibited immunoreactivity with Aβ plaques in 5xFAD mouse brain slices (Figures S4–S12).

The component β-hairpin peptides of the 2AT and KLT trimers contain fragments from the central and *C*-terminal regions of the Aβ peptide but do not contain the β-hairpin loops that would comprise $A\beta_{24–29}$ and $A\beta_{23–29}$ on β-hairpins of full-length Aβ. We recently reported the generation and study of polyclonal antibodies raised against an analogue of 2AT that contains the $A\beta_{24–29}$ loops.[33] Unlike the 2AT and KLT mAbs reported in the current paper, these polyclonal antibodies strongly recognize pathological Aβ in brain slices from individuals who lived with Alzheimer's disease as well as brain slices from 5xFAD mice. These findings taken together with the findings in this paper, suggest that the β-hairpin loop may be an important structure for generating antibodies against Aβ oligomer mimics that bind biogenic Aβ assemblies.

CONCLUSIONS

Elucidating the structures of Aβ oligomers that form in the brain presents an immense unmet challenge in Alzheimer's disease research. The "bottom-up" approach described here holds the promise of using mAbs to correlate the high-resolution structures of Aβ oligomer

mimics with the structures of Aβ oligomers in the brain. Single B-cell sorting of PBMCs from rabbits immunized with the Aβ-derived oligomer mimics 2AT and KLT affords mAbs that are selective for epitopes unique to each oligomer mimic. Two of the mAbs (RBAT_120 and RB2AT_167) are distinctly conformation-specific, respectively exhibiting selectivity for early $A\beta_{42}$ aggregates and mature $A\beta_{42}$ fibrils *in vitro.* Many of the other mAbs also exhibit selectivity for aggregated $A\beta_{42}$ *in vitro,* but appear to be weaker binders. These observations suggest that various forms of aggregated $A\beta_{42}$ share epitopes with 2AT and KLT.

Despite the *in vitro* recognition of $A\beta_{42}$, the 2AT and KLT mAbs did not recognize biogenic Aβ species in the immunostaining studies on brain slices from 5xFAD mice. These observations suggests that the epitopes may not be exposed in the fixed brain tissue or that the epitopes recognized *in vitro* are not formed by Aβ *in'vivo.* High-resolution X-ray crystallographic structures of the Fab-trimer complexes may yield additional insights. We have thus far been unable to obtain X-ray crystallographic structures of the Fab-trimer complexes. We have attempted to elucidate the X-ray crystallographic structure of the RB2AT_87 Fab bound to 2AT, but we observed only the Fab without electron density for the trimer (Figure S12, PDB 8TOO).

The mAbs reported here add to a growing number of amyloid antibodies with refined specificity against distinct Aβ conformations. The mAb 24B3 reported by Murakami *et al.,* is highly specific for a toxic $A\beta_{42}$ dimer with a turn at GIU_{22} and A_{sp23} and was isolated from mouse hybridomas.[34] A polyclonal rabbit antibody that is selective for $A\beta_{42}$ was also recently identified and characterized by Colvin *et al.*[35] In addition, several anti-Aβ mAbs have been approved as therapeutics or are in late-stage clinical trials, with Aduhelm and Leqembi both recently gaining approval.[36,37,38]

Supplementary Material

Refer to Web version on PubMed Central for supplementary material.

ACKNOWLEDGEMENTS

We thank Dr. Shimako Kawauchi, Dr. Grant MacGregor, and the staff at the University of California Irvine Transgenic Mouse Facility for breeding and genotyping the 5xFAD mice. The authors acknowledge the support of the Chao Family Comprehensive Cancer Center Transgenic Mouse Facility Shared Resource, supported by the National Cancer Institute of the National Institutes of Health under award number P30CA062203. The content is solely the responsibility of the authors and does not necessarily represent the official views of the National Institutes of Health. Use of the Stanford Synchrotron Radiation Lightsource, SLAC National Accelerator Laboratory, is supported by the U.S. Department of Energy, Office of Science, Office of Basic Energy Sciences under Contract No. DE-AC02–76SF00515. The SSRL Structural Molecular Biology Program is supported by the DOE Office of Biological and Environmental Research, and by the National Institutes of Health, National Institute of General Medical Sciences (P30GM133894). The contents of this publication are solely the responsibility of the authors and do not necessarily represent the official views of NIGMS or NIH. We thank the National Institutes of Health (NIH) National Institute on Aging (NIA) for funding (Grant number AG062296).

DATA AVAILABLITY

All data are provided in the manuscript and Supporting Information.

REFERENCES AND NOTES

1. Cline EN; Bicca MA; Viola KL; Klein WL The Amyloid-β Oligomer Hypothesis: Beginning of the Third Decade. J.Alzheimers. Dis. 2018, 64 (si), S567–S610. [PubMed: 29843241]
2. Haass C; Selkoe DJ Soluble Protein Oligomers in Neurodegeneration: Lessons from the Alzheimer's Amyloid Beta-Peptide. Nat. Rev.Mol. Cell Biol. 2007, 8 (2), 101–112. [PubMed: 17245412]
3. Benilova I; Karran E; De Strooper B The Toxic Aβ Oligomer and Alzheimer's Disease: An Emperor in Need of Clothes. Nat. Neurosci. 2012, 15 (3), 349–357. [PubMed: 22286176]
4. Liu P; Reed MN; Kotilinek LA; Grant MKO; Forster CL; Qiang W; Shapiro SL; Reichl JH; Chiang ACA; Jankowsky JL; Wilmot CM; Cleary JP; Zahs KR; Ashe KH Quaternary Structure Defines a Large Class of Amyloid-β Oligomers Neutralized by Sequestration. Cell Rep. 2015, 11 (11), 1760–1771. [PubMed: 26051935]
5. A she KH The Biogenesis and Biology of Amyloid β Oligomers in the Brain. Alzheimers. Dement. 2020, 16 (11), 1561–1567. [PubMed: 32543725]
6. Burdick D; Soreghan B; Kwon M; Kosmoski J; Knauer M; Henschen A; Yates J; Cotman C; Glabe C Assembly and Aggregation Properties of Synthetic Alzheimer's A4/beta Amyloid Peptide Analogs. J.Biol. Chem. 1992, 267 (1), 546–554. [PubMed: 1730616]
7. Soreghan B; Kosmoski J; Glabe C Surfactant Properties of Alzheimer's A Beta Peptides and the Mechanism of Amyloid Aggregation. J.Biol. Chem. 1994, 269 (46), 28551–28554. [PubMed: 7961799]
8. Walsh DM; Lomakin A; Benedek GB; Condron MM; Teplow DB Amyloid Beta-Protein Fibrillogenesis. Detection of a Protofibrillar Intermediate. J. Biol. Chem. 1997, 272 (35), 22364–22372. [PubMed: 9268388]
9. Lambert MP; Barlow AK; Chromy BA; Edwards C; Freed R; Liosatos M; Morgan TE; Rozovsky I; Trommer B; Viola KL; Wals P; Zhang C; Finch CE; Krafft GA; Klein WL Diffusible, Nonfibrillar Ligands Derived from Abeta1-42 Are Potent Central Nervous System Neurotoxins. Proc. Natl. Acad. Sci. U.S. A. 1998, 95 (11), 6448–6453. [PubMed: 9600986]
10. Harper JD; Wong SS; Lieber CM; Lansbury PT Observation of Metastable Abeta Amyloid Protofibrils by Atomic Force Microscopy. Chem. Biol. 1997, 4 (2), 119–125. [PubMed: 9190286]
11. Kayed R; Pensalfini A; Margol L; Sokolov Y; Sarsoza F; Head E; Hall J; Glabe C Annular Protofibrils Are a Structurally and Functionally Distinct Type of Amyloid Oligomer. J. Biol. Chem. 2009, 284 (7), 4230–4237. [PubMed: 19098006]
12. Stine WB Jr; Dahlgren KN; Krafft GA; LaDu MJ In Vitro Characterization of Conditions for Amyloid-Beta Peptide Oligomerization and Fibrillogenesis. J. Biol. Chem. 2003, 278 (13), 11612–11622. [PubMed: 12499373]
13. Bernstein SL; Dupuis NF; Lazo ND; Wyttenbach T; Condron MM; Bitan G; Teplow DB; Shea J-E; Ruotolo BT; Robinson CV; Bowers MT Amyloid-β Protein Oligomerization and the Importance of Tetramers and Dodecamers in the Aetiology of Alzheimer's Disease. Nat. Chem. 2009, 1 (4), 326–331. [PubMed: 20703363]
14. Im D; Kim S; Yoon G; Hyun DG; Eom Y-G; Lee YE; Sohn CH; Choi J-M; Kim HI Decoding the Roles of Amyloid-β (1–42)'s Key Oligomerization Domains toward Designing Epitope-Specific Aggregation Inhibitors. JACSAu 2023, 3 (4), 1065–1075.
15. Kayed R; Head E; Thompson JL; Mclntire TM; Milton SC; Cotman CW; Glabe CG Common Structure of Soluble Amyloid Oligomers Implies Common Mechanism of Pathogenesis. Science 2003, 300 (5618), 486–489. [PubMed: 12702875]
16. Kayed R; Head E; Sarsoza F; Saing T; Cotman CW; Necula M; Margol L; Wu J; Breydo L; Thompson JL; Rasool S; Gurlo T; Butler P; Glabe CG Fibril Specific, Conformation Dependent Antibodies Recognize a Generic Epitope Common to Amyloid Fibrils and Fibrillar Oligomers That Is Absent in Prefibrillar Oligomers.Mo/. Neurodegener. 2007, 2, 18.
17. Kayed R; Canto I; Breydo L; Rasool S; Lukacsovich T; Wu J; Albay R 3rd; Pensalfini A; Yeung S; Head E; Marsh JL; Glabe C Conformation Dependent Monoclonal Antibodies Distinguish Different Replicating Strains or Conformers of Prefibrillar Aβ Oligomers. Mol. Neurodegener. 2010, 5,57. [PubMed: 21144050]

18. Lambert MP; Velasco PT; Chang L; Viola KL; Fernandez S; Lacor PN; Khuon D; Gong Y; Bigio EH; Shaw P; De Felice FG; Krafft GA; Klein WL Monoclonal Antibodies That TargetPathological Assemblies of Abeta. J.Neurochem. 2007,100 (1), 23–35. [PubMed: 17116235]
19. Lasagna-Reeves CA; Glabe CG; Kayed R Amyloid-β AnnularProtofibrils Evade FibrillarFate in AlzheimerDisease Brain. J.Biol. Chem. 2011, 286 (25), 22122–22130. [PubMed: 21507938]
20. Jin M; O'Nuallain B; Hong W; Boyd J; Lagomarsino VN; O'Malley TT; Liu W; Vanderburg CR; Frosch MP; Young-Pearse T; Selkoe DJ; Walsh DM An in Vitro Paradigm to Assess Potential Anti-Aβ Antibodies for Alzheimer's Disease. Nat. Commun. 2018, 9 (1), 2676. [PubMed: 29992960]
21. Krafft GA; Jerecic J; Siemers E; Cline EN ACU193: An Immunotherapeutic Poised to Test the Amyloid β OligomerHypothesis of Alzheimer's Disease. Front. Neurosci. 2022, 16, 848215. [PubMed: 35557606]
22. Kreutzer AG; Guaglianone G; Yoo S; Parrocha CMT; Ruttenberg SM; Malonis RJ; Tong K; Lin Y-F; Nguyen JT; Howitz WJ; Diab MN; Hamza IL; Lai JR; Wysocki VH; Nowick JS Probing Differences among Aβ Oligomers with Two Triangular Trimers Derived from Aβ. Proc. Natl. Acad. Sei. U. S. A. 2023, 120 (22), e2219216120.
23. Kreutzer AG; Yoo S; Spencer RK; Nowick JS Stabilization, Assembly, and Toxicity of Trimers Derived from Aβ. J.Am. Chem. Soc. 2017, 139 (2), 966–975. [PubMed: 28001392]
24. Tiller T; Meffre E; Yurasov S; Tsuiji M; Nussenzweig MC; Wardemann H Efficient Generation of Monoclonal Antibodies from Single Human B Cells by Single Cell RT-PCR and Expression Vector Cloning. J. Immunol.Methods 2008, 329 (1–2), 112–124. [PubMed: 17996249]
25. Malonis RJ; Earnest JT; Kim AS; Angeliadis M; Holtsberg FW; Aman MJ; Jangra RK; Chandran K; Daily JP; Diamond MS; Kielian M; Lai JR Near-Germline Human Monoclonal Antibodies Neutralize and Protect against Multiple Arthritogenic Alphaviruses. Proc. Natl. Acad. Sci. U.S. A. 2021, 118 (37). 10.1073/pnas.2100104118.
26. Rader C; Ritter G; Nathan S; Elia M; Gout I; Jungbluth AA; Cohen LS; Welt S; Old LJ; Barbas CF 3rd. The Rabbit Antibody Repertoire as a Novel Source for the Generation of Therapeutic Human Antibodies. J. Biol. Chem. 2000, 275 (18), 13668–13676. [PubMed: 10788485]
27. Seeber S; Ros F; Thorey I; Tiefenthaler G; Kaluza K; Lifke V; Fischer JAA; Klostermann S; Endl J; Kopetzki E; Pashine A; Siewe B; Kaluza B; Platzer J; Offner S A Robust High Throughput Platform to Generate Functional Recombinant Monoclonal Antibodies Using Rabbit B Cells from Peripheral Blood. PLoS One 2014, 9 (2), e86184. [PubMed: 24503933]
28. Mazor Y; Barnea I; Keydar I; Benhar I Antibody Internalization Studied Using a Novel IgG Binding Toxin Fusion. J.Immunol.Methods 2007, 321 (1–2), 41–59. [PubMed: 17336321]
29. Lefranc M-P; Giudicelli V; Ginestoux C; Jabado-Michaloud J; Folch G; Bellahcene F; Wu Y; Gemrot E; Brochet X; Lane J; Regnier L; Ehrenmann F; Lefranc G; Duroux P IMGT, the International ImMunoGeneTics Information System. Nucleic Acids Res. 2009, 37 (Database issue), D1006–D1012. [PubMed: 18978023]
30. Zhang Z; Liu H; Guan Q; Wang L; Yuan H Advances in the Isolation of Specific Monoclonal Rabbit Antibodies. Front. Immunol. 2017, 8, 494. [PubMed: 28529510]
31. Rossi S; Laurino L; Furlanetto A; Chinellato S; Orvieto E; Canal F; Facchetti F; Dei Tos AP Rabbit Monoclonal Antibodies: A Comparative Study between a Novel Category of Immunoreagents and the Corresponding Mouse Monoclonal Antibodies. Am. J. Clin. Pathol. 2005, 124 (2), 295–302.
32. Kayed R; Glabe CG Conformation-Dependent Anti-Amyloid Oligomer Antibodies. Methods Enzymol. 2006, 413, 326–344. [PubMed: 17046404]
33. Kreutzer AG; Parrocha CMT; Haerianardakani S; Guaglianone G; Nguyen JT; Diab MN; Yong W; Perez-Rosendahl M; Head E; Nowick JS Antibodies Raised against an Aβ Oligomer Mimic Recognize Pathological Features in Alzheimer's Disease and Associated Amyloid-Disease Brain Tissue. bioRxiv, 2023. 10.1101/2023.05.ll.540404.
34. Murakami K; Tokuda M; Suzuki T; Irie Y; Hanaki M; Izuo N; Monobe Y; Akagi K-I; Ishii R; Tatebe H; Tokuda T; Maeda M; Kume T; Shimizu T; Irie K Monoclonal Antibody with Conformational Specificity for a Toxic Conformer of Amyloid β42 and Its Application toward the Alzheimer's Disease Diagnosis. Sci. Rep. 2016, 6, 29038. [PubMed: 27374357]

35. Colvin BA; Rogers VA; Kulas JA; Ridgway EA; Amtashar FS; Combs CK; Nichols MR The Conformational Epitope for a New Aβ42 Protofibril-Selective Antibody Partially Overlaps with the Peptide N-Terminal Region. J. Neurochem. 2017, 143 (6), 736–749. [PubMed: 28881033]

36. Sevigny J; Chiao P; Bussiere T; Weinreb PH; Williams L; Maier M; Dunstan R; Salloway S; Chen T; Ling Y; O'Gorman J; Qian F; Arastu M; Li M; Chollate S; Brennan MS; Quintero-Monzon O; Scannevin RH; Arnold HM; Engber T; Rhodes K; Ferrero J; Hang Y; Mikulskis A; Grimm J; Hock C; Nitsch RM; Sandrock A The Antibody Aducanumab Reduces Aβ Plaques in Alzheimer's Disease. Nature 2016, 537 (7618), 50–56. [PubMed: 27582220]

37. Englund H; Sehlin D; Johansson A-S; Nilsson LNG; Gellerfors P; Paulie S; Lannfelt L; Pettersson FE Sensitive ELISA Detection of Amyloid-Beta Protofibrils in Biological Samples. J. Neurochem. 2007, 103 (1), 334–345. [PubMed: 17623042]

38. van Dyck CH; Swanson CJ; Aisen P; Bateman RJ; Chen C; Gee M; Kanekiyo M; Li D; Reyderman L; Cohen S; Froelich L; Katayama S; Sabbagh M; Vellas B; Watson D; Dhadda S; Irizarry M; Kramer LD; Iwatsubo T Lecanemab in Early Alzheimer's Disease. N. Engl. J. Med. 2023, 355(1), 9–21.

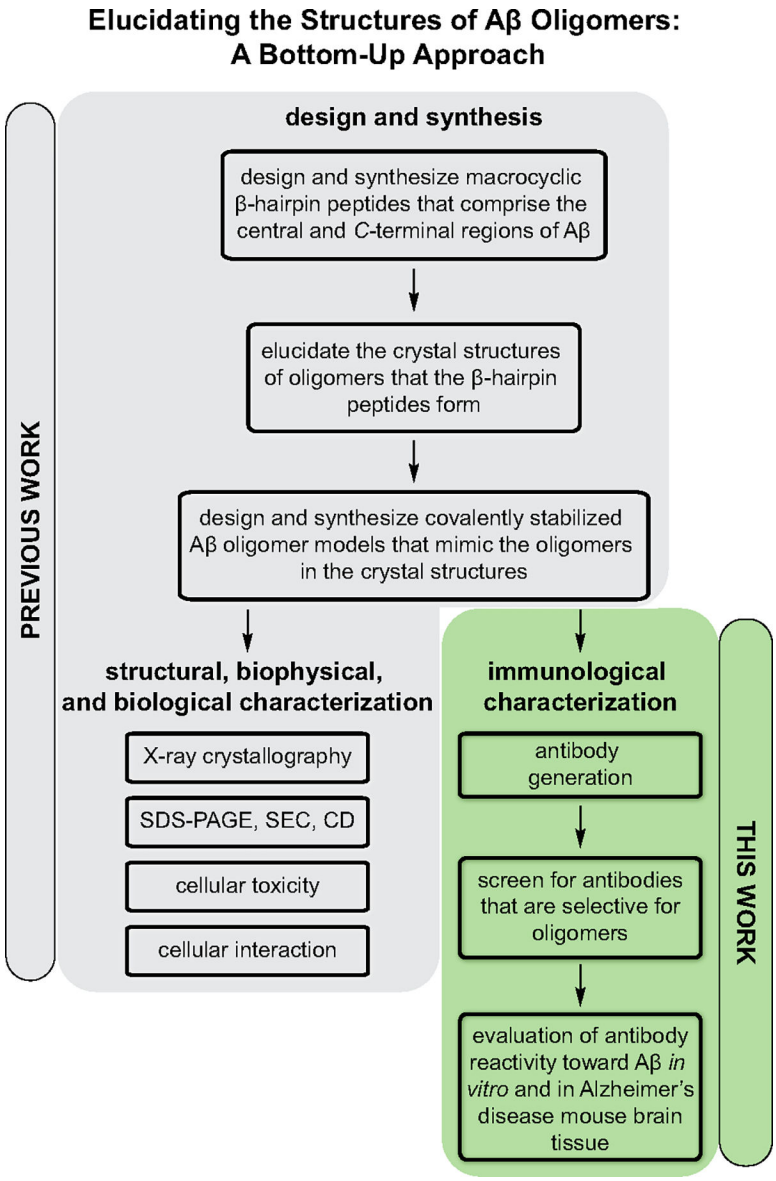

Figure 1.
A bottom-up approach for understanding the structures of Aβ oligomers.

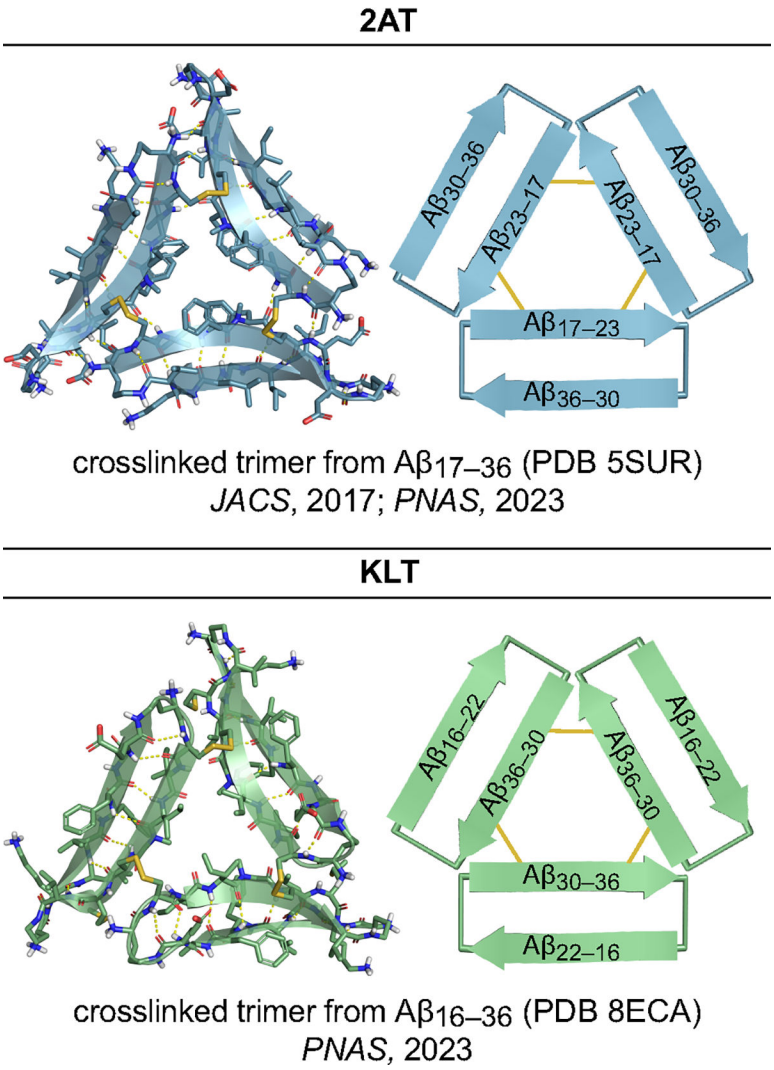

Figure 2.

X-ray crystallographic structures and cartoon depictions of2A T (top) and KLT (bottom).[22,23]

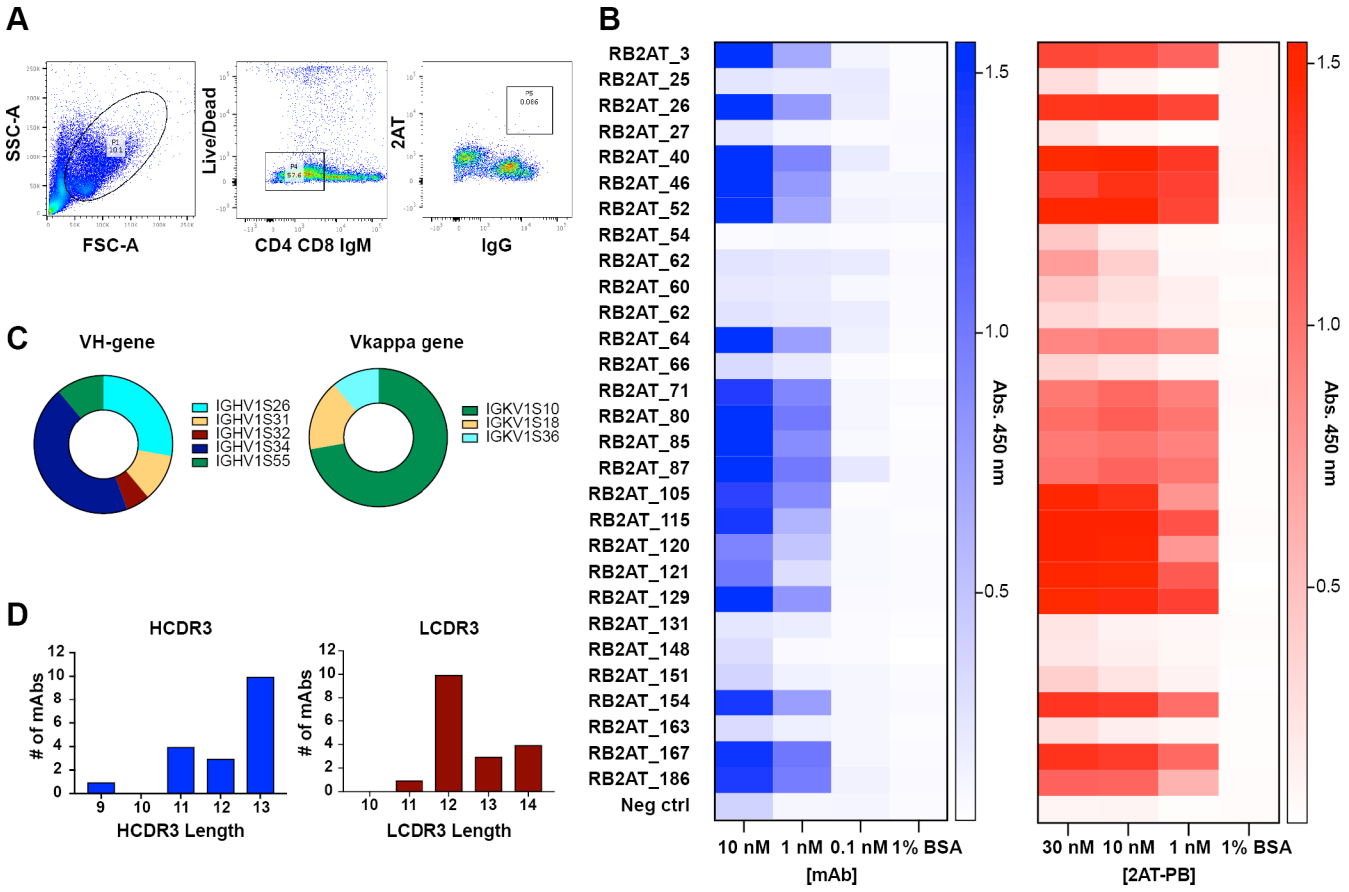

Figure 3.

Isolation and characterization of mAbs targeting 2AT. ***(A)*** Single cell sorting to identify $2AT^{+}/IgG^{+}$ B cells. PBMCs were sorted for size and granularity (forward and side scatter, FSC-A and SSC-A) consistent with single lymphocytes. The live, $CD4^{-}$ $CD8^{-}$ IgM^{-} population was carried forward (to eliminate non-B-cell, non-IgG lymphocytes), then positively gated for $2AT^{+}/IgG^{+}$ B cells. ***(B)*** Screening of mAbs for binding to 2AT by ELISA. In blue, three mAb concentrations are tested with 2AT as the immobilized target. In red, three 2AT-PB concentrations are tested with the mAb immobilized. ***(C)*** Distribution of heavy chain and light chain originating germline V segments. V gene families were represented in both the heavy (IGHV) and light (IGKV) chains. ***(D)*** Distribution of HCDR3 (blue) and LCDR3 (red) loop lengths. The diverse originating germline segments (C) along with distribution of CDR3 lengths (D) among the mAb panel suggests a broad array of interaction modes.

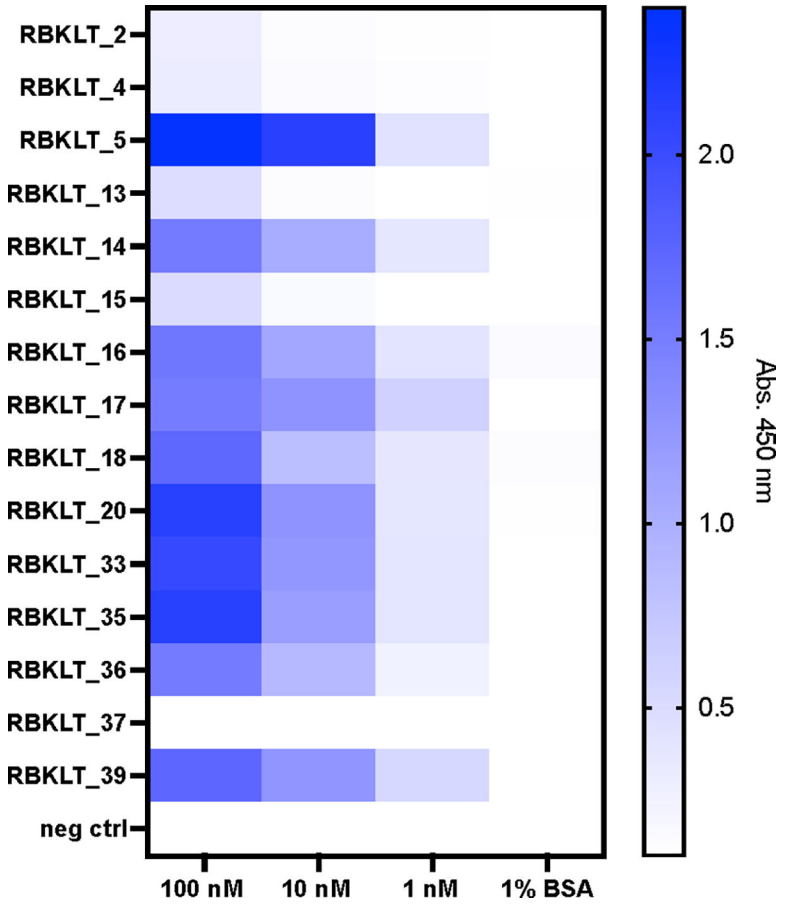

Figure 4.

Screening of mAbs for binding to KLT by ELISA. Three mAb concentrations are tested with KLT as the immobilized target.

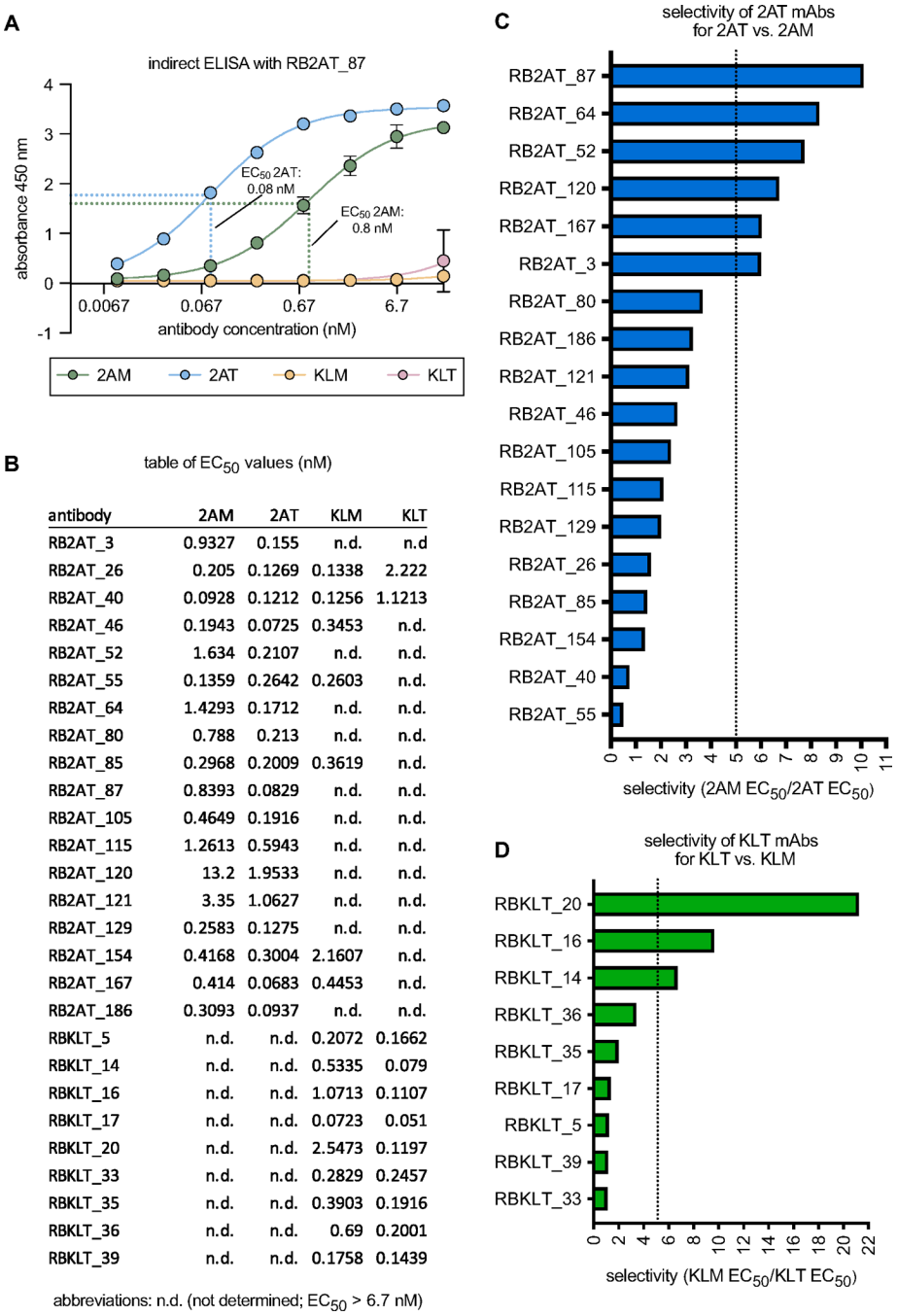

antibody	2AM	2AT	KLM	KLT
RB2AT_3	0.9327	0.155	n.d.	n.d
RB2AT_26	0.205	0.1269	0.1338	2.222
RB2AT_40	0.0928	0.1212	0.1256	1.1213
RB2AT_46	0.1943	0.0725	0.3453	n.d.
RB2AT_52	1.634	0.2107	n.d.	n.d.
RB2AT_55	0.1359	0.2642	0.2603	n.d.
RB2AT_64	1.4293	0.1712	n.d.	n.d.
RB2AT_80	0.788	0.213	n.d.	n.d.
RB2AT_85	0.2968	0.2009	0.3619	n.d.
RB2AT_87	0.8393	0.0829	n.d.	n.d.
RB2AT_105	0.4649	0.1916	n.d.	n.d.
RB2AT_115	1.2613	0.5943	n.d.	n.d.
RB2AT_120	13.2	1.9533	n.d.	n.d.
RB2AT_121	3.35	1.0627	n.d.	n.d.
RB2AT_129	0.2583	0.1275	n.d.	n.d.
RB2AT_154	0.4168	0.3004	2.1607	n.d.
RB2AT_167	0.414	0.0683	0.4453	n.d.
RB2AT_186	0.3093	0.0937	n.d.	n.d.
RBKLT_5	n.d.	n.d.	0.2072	0.1662
RBKLT_14	n.d.	n.d.	0.5335	0.079
RBKLT_16	n.d.	n.d.	1.0713	0.1107
RBKLT_17	n.d.	n.d.	0.0723	0.051
RBKLT_20	n.d.	n.d.	2.5473	0.1197
RBKLT_33	n.d.	n.d.	0.2829	0.2457
RBKLT_35	n.d.	n.d.	0.3903	0.1916
RBKLT_36	n.d.	n.d.	0.69	0.2001
RBKLT_39	n.d.	n.d.	0.1758	0.1439

abbreviations: n.d. (not determined; EC_{50} > 6.7 nM)

Figure 5.

ELISA of the 2AT and KLT mAbs against 2AM, 2AT, KLM, and KLT. ***(A)*** Representative data from an indirect ELISA of 2AT mAb87. ***(B)*** Table listing the EC_{50} values for each of the 2AT and KLT mAbs. EC_{50} values much greater than the highest concentration of mAh tested (3 μg/mL) are listed as not determined (n.d.). ***(C)*** Selectivity of the 2AT mAbs for 2AT over 2AM. The selectivity of each 2AT mAh was determined by calculating the quotient of the 2AM EC_{50} value and the 2AT EC_{50} value. The dotted line indicates 2AT mAbs that are greater than fivefold more selective for the trimer 2AT than the monomer

2AM. ***(D)*** Selectivity of the KLT mAbs for KLT over KLM. The selectivity of each KLT mAh was determined by calculating the quotient of the KLM EC_{50} value and the KLT EC_{50} value. The dotted line indicates KLT mAbs that are greater than fivefold more selective for the trimer KLT than the monomer KLM.

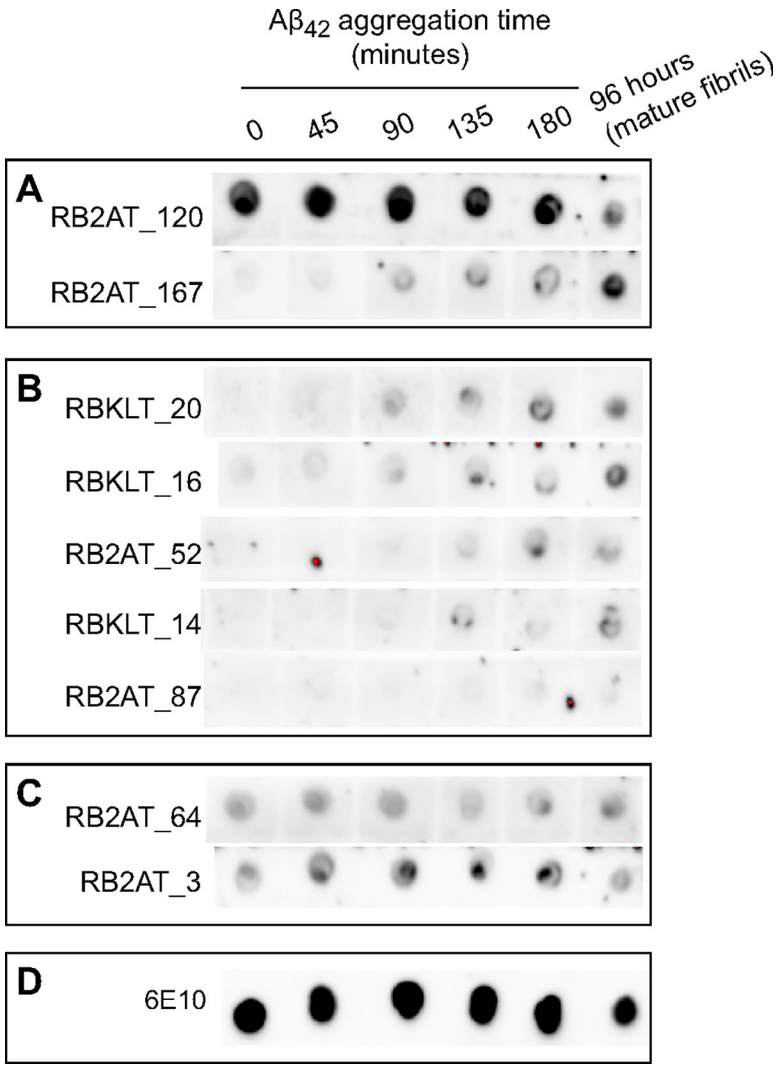

Figure 6.

Dot blot assay of select 2AT and KLT mAbs (A–C) and the control anti-Aβ antibody 6E10 (D) against $A\beta_{42}$ aggregated over time.